

CEP41 is mutated in Joubert syndrome and is required for tubulin glutamylation at the cilium

Ji Eun Lee^{1,2}, Jennifer L Silhavy^{1,2}, Maha S Zaki³, Jana Schroth^{1,2}, Stephanie L Bielas^{1,2}, Sarah E Marsh^{1,2}, Jesus Olvera^{1,2}, Francesco Brancati^{4,5}, Miriam Iannicelli⁴, Koji Ikegami⁶, Andrew M Schlossman^{1,2}, Barry Merriman⁷, Tania Attié-Bitach⁸, Clare V Logan⁹, Ian A Glass^{10,11}, Andrew Cluckey¹², Carrie M Louie^{1,2}, Jeong Ho Lee^{1,2}, Hilary R Raynes^{13–15}, Isabelle Rapin^{13–15}, Ignacio P Castroviejo¹⁶, Mitsutoshi Setou⁶, Clara Barbot¹⁷, Eugen Boltshauser¹⁸, Stanley F Nelson⁷, Friedhelm Hildebrandt¹², Colin A Johnson⁹, Daniel A Doherty^{10,11}, Enza Maria Valente^{4,19} & Joseph G Gleeson^{1,2}

Tubulin glutamylation is a post-translational modification that occurs predominantly in the ciliary axoneme and has been suggested to be important for ciliary function^{1,2}. However, its relationship to disorders of the primary cilium, termed ciliopathies, has not been explored. Here we mapped a new locus for Joubert syndrome (JBTS)³, which we have designated as JBTS15, and identified causative mutations in CEP41, which encodes a 41-kDa centrosomal protein⁴. We show that CEP41 is localized to the basal body and primary cilia, and regulates ciliary entry of TLL6, an evolutionarily conserved polyglutamylase enzyme⁵. Depletion of CEP41 causes ciliopathy-related phenotypes in zebrafish and mice and results in glutamylation defects in the ciliary axoneme. Our data identify CEP41 mutations as a cause of JBTS and implicate tubulin post-translational modification in the pathogenesis of human ciliary dysfunction.

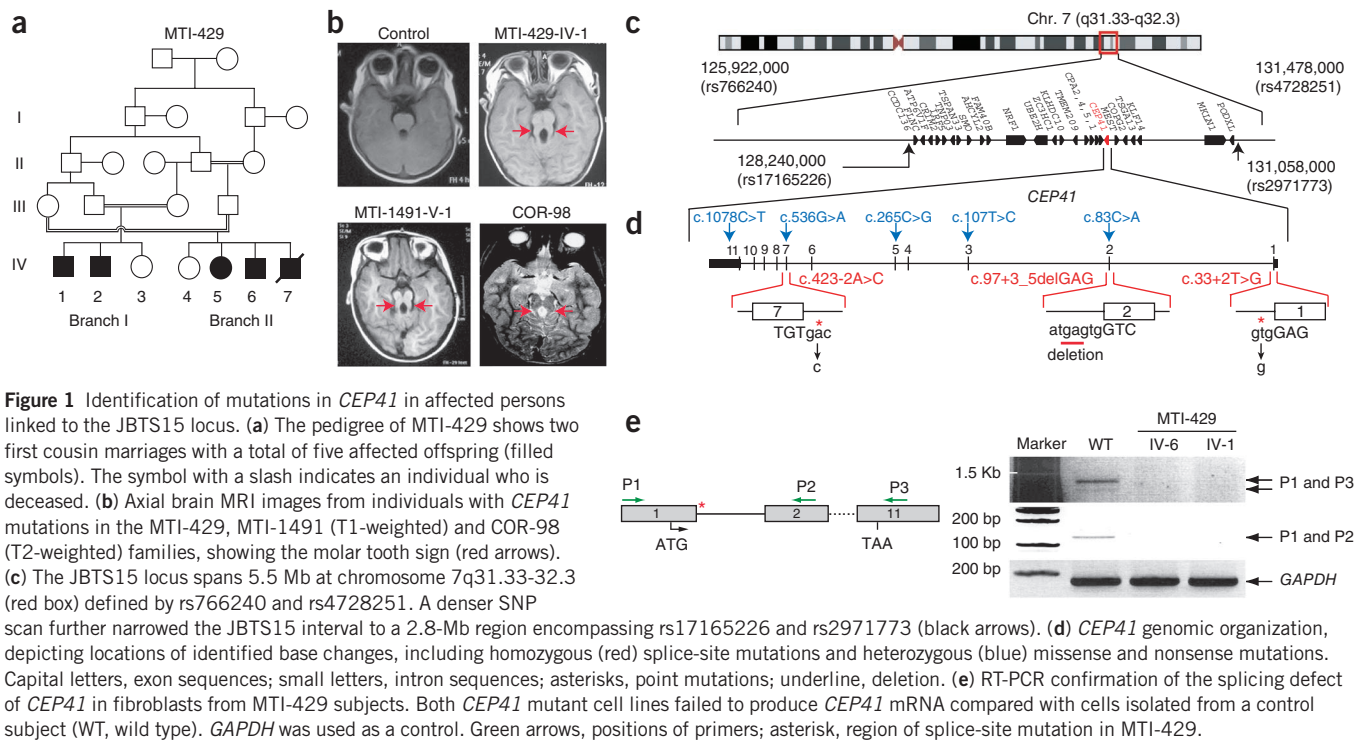
Joubert syndrome (JBTS MIM 213300) is characterized by cerebellar hypoplasia and neurological features, including ataxia, psychomotor delay and oculomotor apraxia with a pathognomonic ‘molar tooth sign’ on brain imaging. JBTS is frequently accompanied by various multi-organ signs and symptoms, including retinal dystrophy, nephronophthisis, liver fibrosis and polydactyly, conditions that are associated with disorders of the ciliopathy spectrum of diseases that include

Meckel-Gruber Syndrome (MKS), Bardet-Biedl syndrome (BBS) and nephronophthisis (NPHP). Although several causative genes have been found for these disorders, they account for less than 50% of cases^{6,7}. We recruited a consanguineous two-branch Egyptian family (MTI-429) with five affected members (Fig. 1a,b and Table 1). We excluded linkage to previously identified JBTS-associated loci using a panel of highly informative markers. Analysis of the family using the Illumina Linkage IVb SNP mapping panel identified a 5-Mb region of linkage to chromosome 7q31.33–32.3 with a peak multipoint logarithm of odds (LOD) score of 3.71, which we have defined as the JBTS15 locus. Haplotype analysis indicated that a candidate interval between the rs766240 and rs4728251 SNPs represented the peak of highest significance (Supplementary Fig. 1a,b).

To further narrow the interval, we reanalyzed MTI-429 samples with the denser Affymetrix 250K NspI SNP array by applying a linkage-free, identity-by-descent (IBD) model⁸. The combination of the two SNP linkage analyses identified a 2.8-Mb IBD interval between rs17165226 and rs2971773 that contains 26 genes (Fig. 1c). Direct sequence analyses of candidate genes within the interval led to the identification of a homozygous c.33+2T>G nucleotide change in CEP41 (NM_018718), which was predicted to abolish the consensus splice-donor site from exon 1 of the CEP41 gene (Fig. 1d and Supplementary Fig. 2a). To determine whether this mutation causes a splicing defect, we evaluated CEP41 transcripts from primary fibroblasts that were isolated from

¹Department of Neurosciences, Howard Hughes Medical Institute, University of California, San Diego, La Jolla, California, USA. ²Neurogenetics Laboratory, Institute for Genomic Medicine, Department of Pediatrics, University of California, San Diego, La Jolla, California, USA. ³Clinical Genetics Department, Human Genetics and Genome Research Division, National Research Centre, Dokki, Egypt. ⁴Casa Sollievo della Sofferenza (CSS) Hospital, CSS-Mendel Laboratory, San Giovanni Rotondo, Italy. ⁵Department of Biopathology and Diagnostic Imaging, Medical Genetics Unit, Tor Vergata University, Rome, Italy. ⁶Department of Cell Biology and Anatomy, Hamamatsu University School of Medicine, Hamamatsu, Japan. ⁷Department of Human Genetics, Pathology and Laboratory Medicine, David Geffen School of Medicine, University of California, Los Angeles, Los Angeles, California, USA. ⁸Département de Génétique, Institut National de la Santé et de la Recherche Médicale (INSERM) U781, Hôpital Necker-Enfants Malades, Université Paris Descartes, Paris, France. ⁹Section of Ophthalmology and Neurosciences, Leeds Institute of Molecular Medicine, St James's University Hospital, Leeds, UK. ¹⁰Department of Pediatrics, Division of Developmental Medicine, University of Washington, Seattle Children's Hospital, Seattle, Washington, USA. ¹¹Division of Genetic Medicine, University of Washington, Seattle Children's Hospital, Seattle, Washington, USA. ¹²Department of Pediatrics and Communicable Diseases, Howard Hughes Medical Institute, University of Michigan, Ann Arbor, Michigan, USA. ¹³Saul R. Korey Department of Neurology, Albert Einstein College of Medicine, New York, New York, USA. ¹⁴Department of Pediatrics, Albert Einstein College of Medicine, New York, New York, USA. ¹⁵Rose F. Kennedy Intellectual and Developmental Disabilities Research Center, Albert Einstein College of Medicine, New York, New York, USA. ¹⁶Pediatric Neurology Service, University Hospital La Paz, Madrid, Spain. ¹⁷Serviço de Neuropediatria, Hospital de Crianças Maria Pia, Porto, Portugal. ¹⁸Department of Pediatric Neurology, University Children's Hospital of Zürich, Zurich, Switzerland. ¹⁹Department of Medical and Surgical Pediatric Sciences, University of Messina, Messina, Italy. Correspondence should be addressed to J.G.G. (jogleeson@ucsd.edu).

Received 28 June 2011; accepted 14 December 2011; published online 15 January 2012; doi:10.1038/ng.1078



MTI-429 family members (MTI-429-IV-1 and MTI-429-IV-6). The RT-PCR result showed an absence of mature *CEP41* mRNA products in cells from both individuals, which can probably be attributed to nonsense-mediated decay (Fig. 1e).

We next screened an additional 832 individuals with ciliopathy (720 with JBTS and 112 with MKS, many of whom were excluded for mutations in known ciliopathy genes) by directly sequencing *CEP41* and found two additional consanguineous families with homozygous mutations, including c.97+3_5delGAG in an Egyptian family with JBTS (MTI-1491) and c.423-2A>C in a Portuguese family with JBTS (COR-98) (Fig. 1b–d and Supplementary Fig. 2a). These mutations were predicted to abolish the consensus splice-donor site from exon 2 and the splice-acceptor site from exon 7, respectively. Moreover, we confirmed that the mutation in MTI-1491 led to skipping of exon 2, thereby generating a premature stop in exon 3 (Supplementary Fig. 2b). In addition to the individuals with JBTS, the MTI-1491 family included one family member with a phenotype consistent with BBS who lacked the pathognomonic molar tooth sign, and this individual was heterozygous for the c.97+3_5delGAG mutation (Supplementary Fig. 2b–d), suggesting that *CEP41* may modify other ciliopathy conditions. From our cohort screen of families affected with JBTS, we identified additional heterozygous *CEP41* mutations (c.83C>A, c.107T>C, c.265C>G, c.536G>A and c.1078C>T) that alter amino acid residues that are highly conserved among vertebrates or lead to a premature stop codon (Fig. 1d, Supplementary Fig. 2e and Supplementary Table 1). Each of the individuals with *CEP41* mutations was additionally sequenced at the known JBTS-associated genes, and four were found to harbor an additional heterozygous, potentially deleterious variant. It is notable that all homozygous mutations in *CEP41* were splice-site mutations and were identified only in subjects with JBTS, whereas heterozygous mutations were present in several ciliopathies, including BBS and MKS. Our findings suggest that constitutive disruptions of *CEP41* result in JBTS, but *CEP41* may also serve as a modifier in the broader class of ciliopathies.

The *CEP41* gene has been poorly characterized except for expression analysis in human organs, including brain, testis and kidney⁹. *CEP41* encodes a 41-kDa centrosomal protein that is predicted to contain two coiled-coil domains and a rhodanese-like domain (RHOD), which is structurally related to the catalytic subunit of the Cdc25 class of phosphatases¹⁰. However, we found that the CEP41 protein lacks phosphatase activity in an *in vitro* *p*-nitrophenylphosphate (pNPP) phosphatase assay (data not shown). The RHOD domain may therefore be an enzymatically inactive version similar to RHOD domains previously described in other proteins¹⁰ that function in protein interactions.

We next examined *CEP41* gene expression at the mRNA level and CEP41 protein subcellular localization. In zebrafish, *cep41* was expressed in various ciliary organs, including Kupffer's vesicle, ear and heart, as well as brain and kidney, the regions that are predominantly affected in JBTS (Fig. 2a and Supplementary Fig. 3). In several ciliated cell lines, such as mouse inner medullary collecting duct cells (IMCD3) and human retinal pigment epithelial cells (hTERT-RPE1), endogenous CEP41 protein was predominantly noted at the centrioles and cilia (Fig. 2b). The cilia-associated expression and localization of CEP41 prompted us to assess a possible role for this protein in cilia-related function. Accordingly, we performed knockdown experiments using translation-blocking morpholino antisense oligonucleotides (MOs) in zebrafish. In embryos injected with *cep41* MO (morphants), we observed peripheral heart edema and tail defects along with ciliopathy-related phenotypes, including hydrocephalus, abnormal ear otolith formation and smaller eyes^{11–14} (Supplementary Fig. 4a,b). We also found that injection of *cep41* MO induced a decrease in production of the protein, with dose-dependent phenotypic severity in the embryos (Supplementary Fig. 4b,c).

Cilia of Kupffer's vesicle, a structure that corresponds to the mammalian embryonic node, are essential to mediate lateral asymmetry¹⁵. Accordingly, defects in left-right asymmetry of the heart, a well-established ciliopathy phenotype in mammals, has been noted

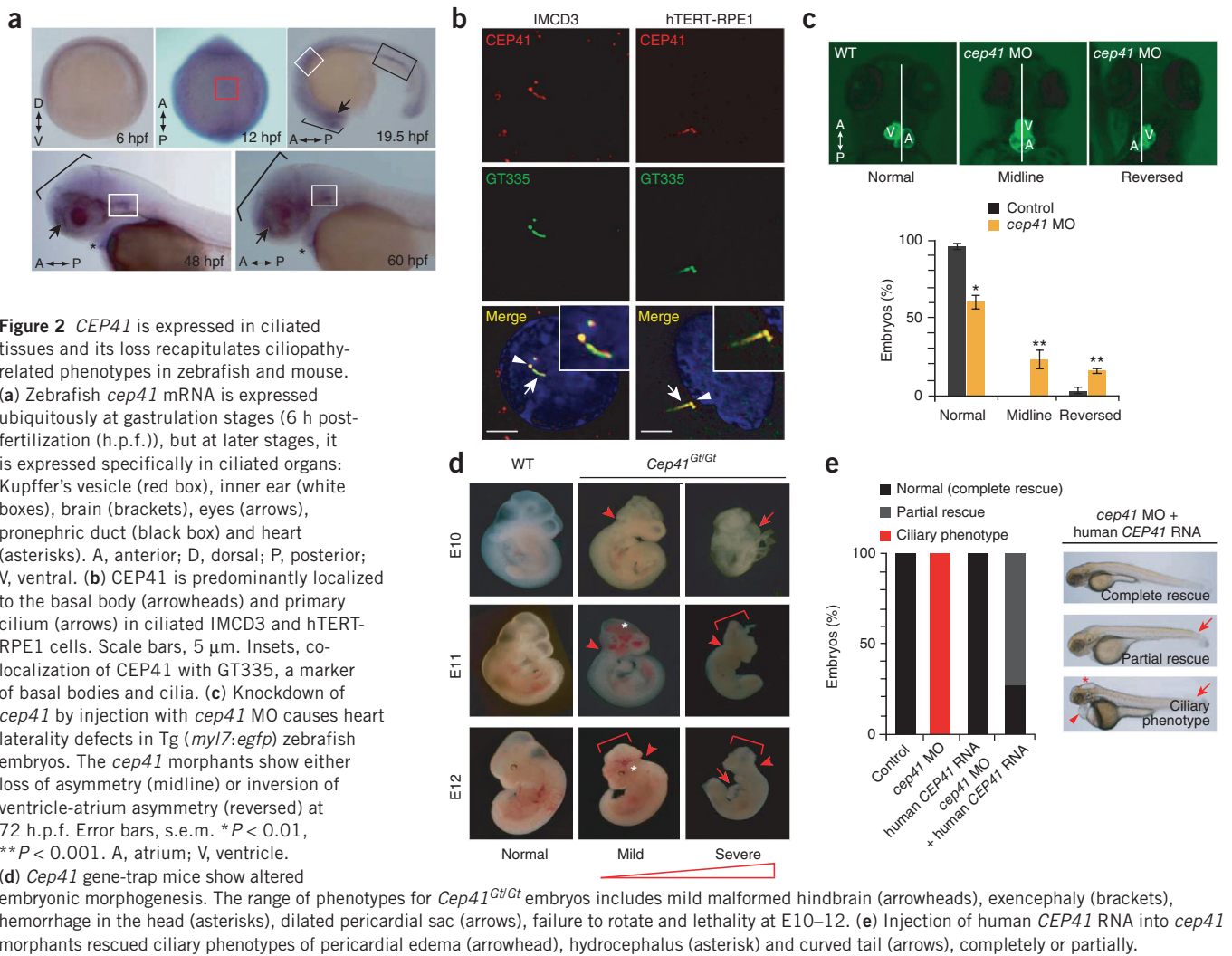
in zebrafish^{16–18}. To examine whether *cep41* depletion resulted in a heart laterality phenotype, we injected *cep41* MO into Tg(*myl7:egfp*) zebrafish, a myocardium-specific transgenic reporter line, and found defects such as inversion or failure to develop asymmetry of the ventricle and atrium (Fig. 2c). We also generated a *Cep41* knockout mouse line using a gene trap strategy (Supplementary Fig. 5a–c)

and characterized its phenotype at embryonic days 10–13 (E10–E13). The homozygous *Cep41*^{Gt/Gt} embryos showed a range of phenotypes: malformed hindbrain, exencephaly, brain hemorrhage, dilated pericardial sac and lethality, as well as unexpected normal development in some homozygous mutants (Fig. 2d, Supplementary Fig. 5d,e and Supplementary Table 2). Although exencephaly, dilated heart

Table 1 Summary of clinical features of individuals with homozygous *CEP41* mutations

Demographic information	MTI-429-IV-1	MTI-429-IV-2	MTI-429-IV-5	MTI-429-IV-6	MTI-429-IV-7	MTI-1491-V-2	MTI-1491-V-3	COR-98
Family ID	MTI-429-IV-1	MTI-429-IV-2	MTI-429-IV-5	MTI-429-IV-6	MTI-429-IV-7	MTI-1491-V-2	MTI-1491-V-3	COR-98
Country of origin	Egypt	Egypt	Egypt	Egypt	Egypt	Egypt	Egypt	Portugal
Sex	M	M	F	M	M	F	F	M
Death	N	N	N	N	N	Died at 7 days	N	N
Documented consanguinity	Y	Y	Y	Y	Y	Y	Y	Y
Neurological signs								
Hypotonia/ataxia	Y	Y	Y	Y	Y	Y	Y	Y
Psychomotor delay	Y	Y	Y	Y	N/A	Y	Y	Y
Mental retardation	Mild	Borderline	Borderline	Borderline	N/A	Y	Y	Y
Oculomotor apraxia	Y	Y	N	N	N/A	Y	Y	N
Breathing abnormalities	N	N	N	N	Y	Y	Y	N
Head circumference	50th percentile	50th percentile	50th percentile	50th percentile	75th percentile	50th percentile	50th percentile	N/A
Ocular signs								
Retinopathy	N	N	N	N	U	N	N	Y
Other abnormalities	B ptosis	U ptosis and leukoma	U ptosis	N	N	U ptosis, squint, leukoma	B squint and leukoma	N
Coloboma	N	N	N	N	U	N	N	N
Renal signs								
NPHP/UCD	N	N	N	N	U	N	N	N
Kidney ultrasound	N	N	N	N	N	N	N	N
Other organs								
Liver abnormalities	N	N	N	N	M	N	N	N
Polydactyly	N	N	U postaxial	U postaxial	B postaxial	N	U postaxial	Y
Other abnormalities	GHD, MP	GHD, MP	N	MP	AG, MP, hypoplastic scrotum	N	N	N
MRI reading								
MTI	Y	Y	Y	Y	Y	Y	Y	Y
Other abnormalities	N	N	N	N	N	N	N	N
<i>CEP41</i> mutation analysis								
Exon(s)	1					2		7
Hetero/Homozygous	Homozygous					Homozygous		Homozygous
Nucleotide change	c.33+2T>G					c.97+3_5delGAG		c.423-2A>C
Amino acid change	Splice site					Splice site		Splice site
Amino acid consequence	Premature stop					Premature stop		Predicted premature stop
Comprehensive JSRD genetic screening								
Linkage	Linkage to chromosome 7 (q31.33-q32.3)					Linkage negative to <i>AHI1</i> , <i>TMEM67</i> and <i>TMEM138-TMEM216</i>		Linkage negative to <i>AHI1</i> , <i>TMEM67</i> and <i>TMEM138-TMEM216</i>
Additional gene with PDSV	None					None		<i>CEP290</i>
Exon								31
Heterozygous/homozygous								Heterozygous
Nucleotide change								c.3626C>G
Amino acid change								p.Ser1209Cys
Amino acid consequence								Neutral to neutral
In NCBI SNP database								No

AG, ambiguous genitalia; B, bilateral; F, female; GHD, growth hormone deficiency; M, male; MP, micropenis; MTI, molar tooth on imaging; N/A, not available or not applicable; NPHP, nephronophthisis; PDSV, potentially deleterious sequence variant; U, unilateral; UCD, urinary concentrating defect.

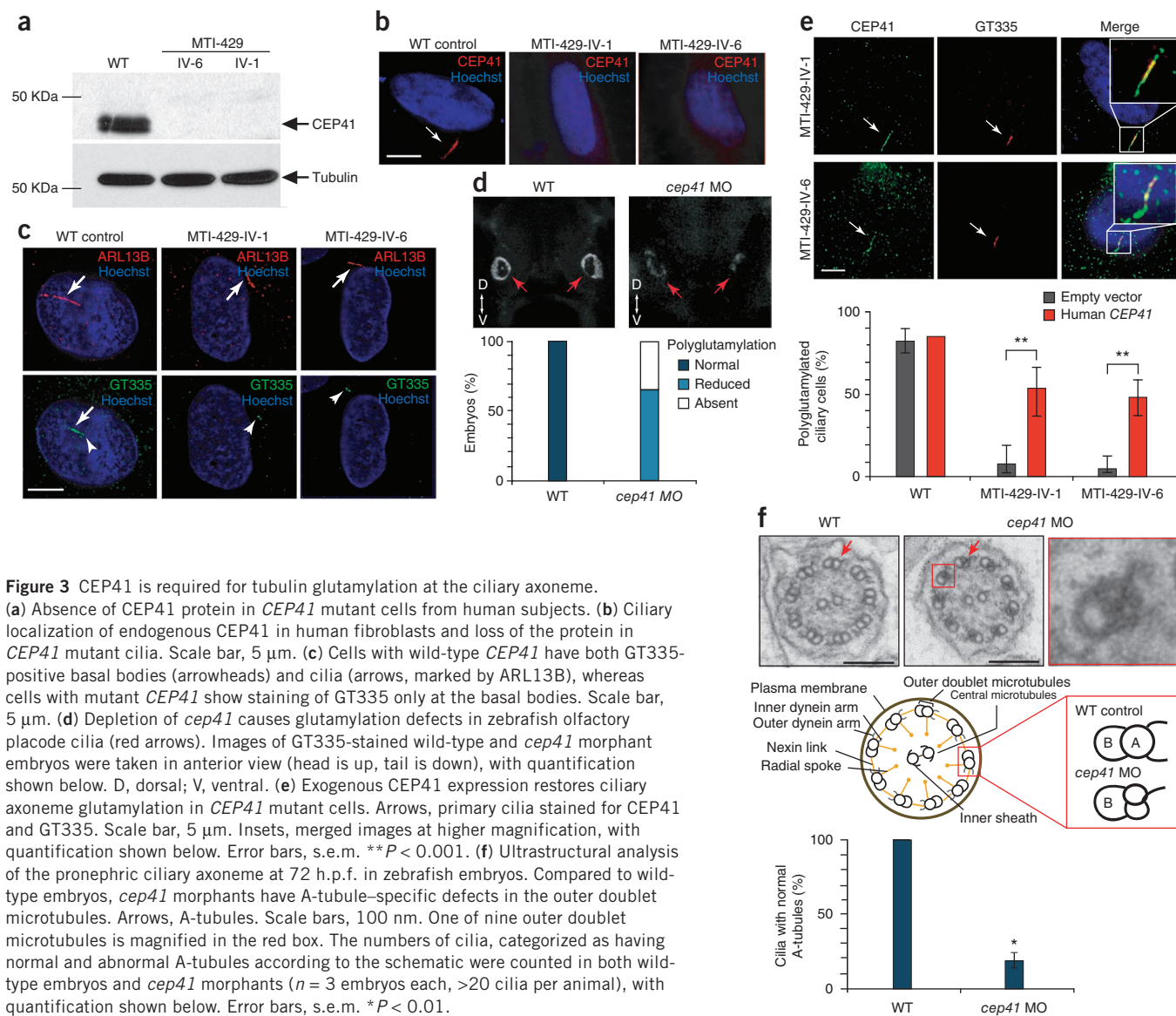


and embryonic lethality suggest possible ciliary roles of *Cep41* in the mouse^{16,19,20}, the phenotypic variability, including the occurrence of normal development, suggests the presence of extragenic phenotypic modifiers. We attempted a genetic rescue using human *CEP41* in zebrafish *cep41* morphants and found partial rescue of the cilia-associated morphant phenotype (Fig. 2e). These data suggest that *CEP41* potentially has an evolutionarily conserved role in ciliary function.

To explore the possible roles of *CEP41*, we examined primary cultured fibroblasts from human subjects (MTI-429-IV-1 and MTI-429-IV-6). We first tested whether *CEP41* mutant cells were devoid of *CEP41* protein. Consistent with RT-PCR results (Fig. 1e), neither fibroblast line produced detectable *CEP41*, showing that these mutant cells are nearly null for *CEP41* (Fig. 3a,b). To examine the effect of *CEP41* loss on cilia assembly, we induced ciliogenesis using serum starvation-mediated cell cycle arrest in confluent cells and visualized cilia by co-immunostaining with antibodies to ARL13B (a cilia marker)²¹ and GT335 (a centriole and cilia marker)²². In control fibroblasts with wild-type *CEP41*, cilia were evident in 70% of the total stained cells by 48 h and 72 h of serum starvation, and nearly all co-stained with both markers (Fig. 3c and Supplementary Fig. 6). However, in the *CEP41* mutant fibroblasts, cilia were stained positively with ARL13B but not with GT335 (Fig. 3c). We quantified this

effect and found that, whereas the percentage of ARL13B-positive ciliated cells in the mutant fibroblasts was approximately equal to that in control fibroblasts, the percentage of GT335-positive ciliated cells was substantially reduced in mutant fibroblasts (Supplementary Fig. 6). The antibody to GT335 was originally generated to recognize the glutamylated forms of tubulin (having both mono- and polyglutamylated tubulin)²³. Therefore, the data suggest a potential role of *CEP41* in regulating tubulin glutamylation.

Microtubules are the major structural scaffolds of the ciliary axoneme and undergo several post-translational modifications, including acetylation, detyrosination, glycylation and glutamylation (Supplementary Fig. 7). We therefore tested the effect of *CEP41* deficiency on these tubulin post-translational modifications in human primary fibroblasts and found no defects other than in glutamylation in *CEP41* mutant cells (Supplementary Fig. 8). In addition, immunostaining using PolyE antibody (specific for polyglutamylated tubulin) in mutant fibroblasts indicated that *CEP41* might regulate both tubulin mono- and polyglutamylated tubulin (Supplementary Fig. 9). Concordantly, we observed a defect in tubulin glutamylation as well as a mild reduction in glycylation of the olfactory placode cilia in zebrafish deficient in *cep41* relative to wild-type animals (Fig. 3d and Supplementary Fig. 10). In the human fibroblast lines, forced expression of exogenous *CEP41* in mutant fibroblasts notably increased the



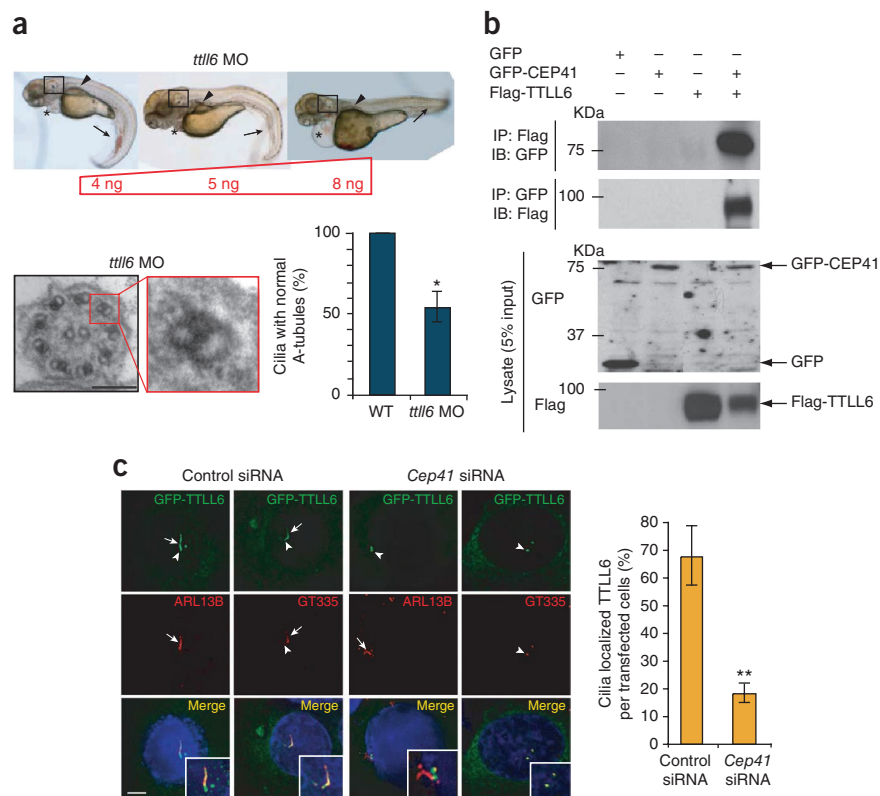
percentage of cells with glutamylated cilia (Fig. 3e), suggesting that glutamylation of the cilium is dependent on the expression of CEP41. Furthermore, we found that cell lines from individuals with mutations in other JBTS-associated genes, including *TMEM216* and *INPP5E*, displayed no such glutamylation defects (data not shown), indicating that the tubulin glutamylation phenotype is not a nonspecific consequence of JBTS-causing mutations. Together, these data show that CEP41 is required for ciliary glutamylation but is not necessary for initial cilia assembly.

Recent studies have shown that defective tubulin post-translational modification is associated with altered ciliary axonemal structure^{24–26}. Accordingly, we investigated whether the CEP41-dysfunctional cilia exhibiting glutamylation defects had an abnormal axonemal structure. Transmission electron microscopy showed that depletion of *cep41* resulted in obvious structural defects in zebrafish renal cilia. Specifically, we found that A-tubules of the outer doublet microtubules of the axoneme were collapsed and/or duplicated (Fig. 3f and Supplementary Fig. 11). Previous studies have suggested that ciliary structural disruption affects ciliary motility^{27,28}; thus, we examined the cilia of Kupffer's vesicle and kidney in zebrafish *cep41* morphants

and found disabled motility of both types of cilia (Supplementary Fig. 12 and Supplementary Videos 1–6). Our data suggest that CEP41 is involved in ciliary structural formation and motility by having an essential role in tubulin glutamylation at the cilium.

We next investigated how CEP41 modulates microtubule post-translational modifications at the ciliary axoneme. We noted that only microtubules of ciliary axonemes showed defective glutamylation, whereas those of centrioles were properly modified in the *CEP41* mutant human fibroblasts (Fig. 3c). Furthermore, the lack of a tubulin tyrosine ligase (TTL) domain in CEP41, which is required for enzymatic activity⁵, implies that it is unlikely to serve as a glutamylase. The main enzymes mediating tubulin glutamylation are members of the conserved TTL-like (TTLL) family⁵. Among several identified TTLL factors, TTLL6 was found to show consistently strong localization to the basal body (the organizing structure at the base of cilium that is derived from a mother centriole) and the cilium (Supplementary Fig. 13). In addition, previous studies have suggested that TTLL6 may be involved in ciliary function in several organisms, including zebrafish^{5,24,29}. We therefore examined the effects of *ttll6* deficiency using a *ttll6* translation-blocking MO³⁰ in zebrafish and observed

Figure 4 CEP41 interacts with TLL6 and is required for TLL6 localization to the cilium. (a) MO-mediated knockdown of zebrafish *tll6* results in ciliary phenotypes, such as abnormal number and/or orientation of ear otolith (boxes), cystic kidney (arrowheads) and peripheral cardiac edema (asterisks) as well as curved tail (arrows) at the different dosages indicated and causes A-tubule-specific defects in the outer doublet microtubules. The numbers of defective cilia were counted in both wild-type embryos and *tll6* morphants ($n = 3$ embryos each, >20 cilia per animal), with quantification shown below. (b) GFP-CEP41 and its associated proteins were immunoprecipitated with antibody to the Flag epitope recognizing Flag-tagged TLL6 from the whole-cell extract (WCE) of cells transfected with this expression construct, with immunoprecipitation in WCE from cells transfected with empty GFP vector serving as a control. In the reciprocal co-immunoprecipitation experiment with antibody to GFP, the interaction between CEP41 and TLL6 was confirmed. (c) Disturbed localization of TLL6 to the cilium following the co-transfection of *Cep41* siRNA with GFP-TLL6 into IMCD3 cells as determined by immunostaining with either GT335 or ARL13B antibody. Arrows, cilia; arrowheads, basal bodies. Scale bar, 5 μm . Cells expressing cilium-localized TLL6 were counted only in siRNA-transfected cells and are quantified in the graph. Error bars, s.e.m. $*P < 0.01$, $**P < 0.001$.



ciliopathy-related morphological phenotypes similar to, although less severe than, what we observed following *cep41* knockdown (Fig. 4a). Additionally, *tll6* morphants showed A-tubule axonemal defects, similar to those of *cep41* morphants (Fig. 4a), along with diverse axonemal structural defects, which were consistent with a previous report³⁰ (data not shown). These data prompted us to test a possible functional relationship between CEP41 and TLL6 by pairwise co-immunoprecipitation. We found that the two proteins were part of a complex (Fig. 4b). We next tested whether CEP41 might function to regulate the transport of TLL6 between the basal body and the cilium as has been suggested for the *fleeer* gene in zebrafish²⁹. Following efficient knockdown of *Cep41* in mouse IMCD cells using siRNA (Supplementary Fig. 14), we found localization of TLL6 restricted mainly to the basal bodies, indicating a block of TLL6 entry into the cilium (Fig. 4c). These data suggest that CEP41 functions in tubulin glutamylation by mediating transport of TLL6 between the basal body and cilium.

Our discovery of CEP41 mutations in persons with JBTS provides the first evidence directly linking defective tubulin glutamylation at the cilium to a human ciliopathy. Consistent with previous studies implicating tubulin post-translational modifications in cilia function^{23,24,31,32}, our data suggest that CEP41-mediated ciliary glutamylation is essential for axonemal formation. Moreover, we found that CEP41 is required for the transport of TLL6 to modulate tubulin glutamylation, although it remains to be determined how these molecules function together. Most likely, these proteins enter through the ciliary diffusion barrier at the transition zone^{33,34} and are then transported along ciliary microtubules by intraflagellar transport motor proteins. Thus, examining whether CEP41 and TLL6 form a complex with other factors at these locations will follow as a future study. Because tubulin glycylation is partially affected in *cep41* morphants and the phenotype of *cep41* morphants is more severe than

that of *tll6* morphants, it is likely that CEP41 modulates other TLL family members^{5,30}. Evidence for this possibility has been described in recent studies that show the involvement of both tubulin glycylation and glutamylation, each regulated by different TLL family members, in maintaining ciliary structure and motility^{30,35–37}.

URLs. USCS Human Genome Browser, <http://www.genome.ucsc.edu/>; ClustalW, <http://www.ebi.ac.uk/Tools/msa/clustalw2/>.

METHODS

Methods and any associated references are available in the online version of the paper at <http://www.nature.com/naturegenetics/>.

Note: Supplementary information is available on the Nature Genetics website.

ACKNOWLEDGMENTS

We thank the Marshfield Clinic Research Foundation, Center for Inherited Disease Research (supported by the US National Institutes of Health and National Heart, Lung, and Blood Institute) for genotyping support. We thank the International JSRD Study Group, E. Bertini and the French Society of Foetal Pathology for subject referrals, J. Meerloo at the UCSD Microscopy Core (P30NS047101), T. Meerloo, Y. Jones, M. Farquhar and the Department of Cellular and Molecular Medicine (CMM) Electron Microscopy Core Facility at UCSD, S. Wirth and B. Willis for mutant mouse generation, C. Janke (Institute Curie Research Center) for GT335 antibody, TLLs plasmids and technical advice, I. Drummond and N. Pathak (Massachusetts General Hospital) for *tll6* MO, M. Gorovsky (University of Rochester) for polyE and polyG antibodies, A.T. Look (Dana-Farber Cancer Institute) for the pCS2+ plasmid, S. Audollent for technical help, and B. Sotak, N. Akizu, A. Crawford, V. Cantagrel and E.-J. Choi for stimulating scientific discussion and comments. This work was supported by the US National Institutes of Health (R01NS048453 and R01NS052455 to J.G.G.; R01DK068306 to F.H.; and R01NS064077 to D.A.D.), the American Heart Association (09POST2250641 to J.E.L.), the Italian Ministry of Health (Ricerca Finalizzata Malattie Rare and Ricerca Corrente 2011), the Telethon Foundation Italy (GGP08145) and the Pierfranco and Luisa Mariani Foundation (to E.M.V.). Research was also supported by grants-in-aid from the Ministry of Education, Culture, Sports, Science and

Technology (MEXT) and the Japan Society for the Promotion of Science (JSPS), (23117517 and 23570209 to K.I.), the Newlife Charity, the Medical Research Council (G0700073), the Sir Jules Thorn Charitable Trust (09/JTA to C.A.J.), l'Agence National pour la Recherche (ANR) (07-MRAR-Fetalciliopathies to T.A.-B.), Simons Foundation Autism Research Initiative (to J.G.G.) and the Howard Hughes Medical Institute (to F.H. and J.G.G.).

AUTHOR CONTRIBUTIONS

J.E.L., M.S.Z. and J.G.G. designed the study and experiments with substantial contributions from B.M. S.F.N. helped with fine mapping. J.L.S., S.L.B., J.O., F.B., M.I., A.M.S., T.A.-B., C.V.L., I.A.G., A.C., F.H., C.A.J., D.A.D. and E.M.V. performed genetic screening. J.E.L., J.L.S., J.S., J.O., F.B., M.I., T.A.-B., I.A.G., D.A.D., C.M.L. and J.H.L. performed mutation analysis. M.S.Z., S.E.M., H.R.R., I.R., I.P.C., E.B., C.B. and E.M.V. identified and recruited subjects. K.I. and M.S. shared critical reagents. J.S. helped with genotyping of mutant mice. J.E.L. performed microscopy, biochemical assays and zebrafish and mouse experiments. J.E.L. and J.G.G. interpreted the data and wrote the manuscript.

COMPETING FINANCIAL INTERESTS

The authors declare no competing financial interests.

Published online at <http://www.nature.com/naturegenetics/>.

Reprints and permissions information is available online at <http://www.nature.com/reprints/index.html>.

- Ikegami, K., Sato, S., Nakamura, K., Ostrowski, L.E. & Setou, M. Tubulin polyglutamylation is essential for airway ciliary function through the regulation of beating asymmetry. *Proc. Natl. Acad. Sci. USA* **107**, 10490–10495 (2010).
- Kubo, T., Yanagisawa, H.A., Yagi, T., Hirono, M. & Kamiya, R. Tubulin polyglutamylation regulates axonemal motility by modulating activities of inner-arm dyneins. *Curr. Biol.* **20**, 441–445 (2010).
- Parisi, M.A. Clinical and molecular features of Joubert syndrome and related disorders. *Am. J. Med. Genet. C. Semin. Med. Genet.* **151C**, 326–340 (2009).
- Andersen, J.S. *et al.* Proteomic characterization of the human centrosome by protein correlation profiling. *Nature* **426**, 570–574 (2003).
- van Dijk, J. *et al.* A targeted multienzyme mechanism for selective microtubule polyglutamylation. *Mol. Cell* **26**, 437–448 (2007).
- Valente, E.M., Brancati, F. & Dallapiccola, B. Genotypes and phenotypes of Joubert syndrome and related disorders. *Eur. J. Med. Genet.* **51**, 1–23 (2008).
- Hildebrandt, F. & Zhou, W. Nephronophthisis-associated ciliopathies. *J. Am. Soc. Nephrol.* **18**, 1855–1871 (2007).
- Lander, E.S. & Botstein, D. Homozygosity mapping: a way to map human recessive traits with the DNA of inbred children. *Science* **236**, 1567–1570 (1987).
- Yamada, T. *et al.* The gene *TSGA14*, adjacent to the imprinted gene *MEST*, escapes genomic imprinting. *Gene* **288**, 57–63 (2002).
- Bordo, D. & Bork, P. The rhodanese/Cdc25 phosphatase superfamily. Sequence-structure-function relations. *EMBO Rep.* **3**, 741–746 (2002).
- Beales, P.L. *et al.* *IFT80*, which encodes a conserved intraflagellar transport protein, is mutated in Jeune asphyxiating thoracic dystrophy. *Nat. Genet.* **39**, 727–729 (2007).
- Gorden, N.T. *et al.* CC2D2A is mutated in Joubert syndrome and interacts with the ciliopathy-associated basal body protein CEP290. *Am. J. Hum. Genet.* **83**, 559–571 (2008).
- Colantonio, J.R. *et al.* The dynein regulatory complex is required for ciliary motility and otolith biogenesis in the inner ear. *Nature* **457**, 205–209 (2009).
- Khanna, H. *et al.* A common allele in *RPGRIP1L* is a modifier of retinal degeneration in ciliopathies. *Nat. Genet.* **41**, 739–745 (2009).
- Essner, J.J., Amack, J.D., Nyholm, M.K., Harris, E.B. & Yost, H.J. Kupffer's vesicle is a ciliated organ of asymmetry in the zebrafish embryo that initiates left-right development of the brain, heart and gut. *Development* **132**, 1247–1260 (2005).
- Nonaka, S. *et al.* Randomization of left-right asymmetry due to loss of nodal cilia generating leftward flow of extraembryonic fluid in mice lacking KIF3B motor protein. *Cell* **95**, 829–837 (1998).
- McGrath, J. & Brueckner, M. Cilia are at the heart of vertebrate left-right asymmetry. *Curr. Opin. Genet. Dev.* **13**, 385–392 (2003).
- Amack, J.D. & Yost, H.J. The T box transcription factor no tail in ciliated cells controls zebrafish left-right asymmetry. *Curr. Biol.* **14**, 685–690 (2004).
- Ross, A.J. *et al.* Disruption of Bardet-Biedl syndrome ciliary proteins perturbs planar cell polarity in vertebrates. *Nat. Genet.* **37**, 1135–1140 (2005).
- Hoover, A.N. *et al.* C2cd3 is required for cilia formation and Hedgehog signaling in mouse. *Development* **135**, 4049–4058 (2008).
- Caspary, T., Larkins, C.E. & Anderson, K.V. The graded response to Sonic Hedgehog depends on cilia architecture. *Dev. Cell* **12**, 767–778 (2007).
- Jurczyk, A. *et al.* Pericentrin forms a complex with intraflagellar transport proteins and polycystin-2 and is required for primary cilia assembly. *J. Cell Biol.* **166**, 637–643 (2004).
- Million, K. *et al.* Polyglutamylation and polyglycylation of α - and β -tubulins during *in vitro* ciliated cell differentiation of human respiratory epithelial cells. *J. Cell Sci.* **112**, 4357–4366 (1999).
- Suryavanshi, S. *et al.* Tubulin glutamylation regulates ciliary motility by altering inner dynein arm activity. *Curr. Biol.* **20**, 435–440 (2010).
- Vogel, P., Hansen, G., Fontenot, G. & Read, R. Tubulin tyrosine ligase-like 1 deficiency results in chronic rhinosinusitis and abnormal development of spermatid flagella in mice. *Vet. Pathol.* **47**, 703–712 (2010).
- Wloga, D. *et al.* Hyperglutamylation of tubulin can either stabilize or destabilize microtubules in the same cell. *Eukaryot. Cell* **9**, 184–193 (2010).
- Becker-Heck, A. *et al.* The coiled-coil domain containing protein CCDC40 is essential for motile cilia function and left-right axis formation. *Nat. Genet.* **43**, 79–84 (2011).
- Zhao, C. & Malicki, J. Genetic defects of pronephric cilia in zebrafish. *Mech. Dev.* **124**, 605–616 (2007).
- Pathak, N., Obara, T., Mangos, S., Liu, Y. & Drummond, I.A. The zebrafish *fleer* gene encodes an essential regulator of cilia tubulin polyglutamylation. *Mol. Biol. Cell* **18**, 4353–4364 (2007).
- Pathak, N., Austin, C.A. & Drummond, I.A. Tubulin tyrosine ligase-like genes *ttl3* and *ttl6* maintain zebrafish cilia structure and motility. *J. Biol. Chem.* **286**, 11685–11695 (2011).
- Gaertig, J. & Wloga, D. Ciliary tubulin and its post-translational modifications. *Curr. Top. Dev. Biol.* **85**, 83–113 (2008).
- Shida, T., Cueva, J.G., Xu, Z., Goodman, M.B. & Nachury, M.V. The major α -tubulin K40 acetyltransferase α TAT1 promotes rapid ciliogenesis and efficient mechanosensation. *Proc. Natl. Acad. Sci. USA* **107**, 21517–21522 (2010).
- Kim, S.K. *et al.* Planar cell polarity acts through septins to control collective cell movement and ciliogenesis. *Science* **329**, 1337–1340 (2010).
- Williams, C.L. *et al.* MKS and NPHP modules cooperate to establish basal body/transition zone membrane associations and ciliary gate function during ciliogenesis. *J. Cell Biol.* **192**, 1023–1041 (2011).
- Rogowski, K. *et al.* Evolutionary divergence of enzymatic mechanisms for posttranslational polyglycylation. *Cell* **137**, 1076–1087 (2009).
- Wloga, D. *et al.* TTL3 is a tubulin glycine ligase that regulates the assembly of cilia. *Dev. Cell* **16**, 867–876 (2009).
- Bulinski, J.C. Tubulin posttranslational modifications: a Pushmi-Pullya at work? *Dev. Cell* **16**, 773–774 (2009).

ONLINE METHODS

Research subjects. The MTI-429 family and additional families were recruited worldwide based upon the presence of at least one individual with a neuro-radiographically proven molar tooth sign associated with any JBTS or related disorder (JSRD) phenotype. Whenever possible, individuals underwent a full diagnostic protocol as previously reported³⁸, and a standardized clinical questionnaire was administered to assess the extent of multi-organ involvement. We used standard methods to isolate genomic DNA from peripheral blood of the affected and unaffected family members after obtaining informed consent from all participants. Human subject research was approved by the Ethics Boards of Leeds (East), CASA Sollievo della Sofferenza Hospital/CSS-Mendel Institute and Hôpital Necker-Enfants Malades, the Human Subjects Division at the University of Washington, the University of Michigan Institutional Review Board and the Human Research Protection Program at the University of California, San Diego.

Genome-wide screen and fine mapping. A 5K whole genome linkage SNP scan was performed with the MTI-429 family using the Illumina Linkage IVb mapping panel³⁹, and analyzed with easyLinkage-Plus software⁴⁰, which runs Allegro version 1.2c in a Windows interface to calculate multipoint LOD scores. Parameters were set to autosomal recessive with full penetrance and disease allele frequency of 0.001. Fine mapping on the pedigree was performed with the Affymetrix 250K NspI SNP array, and data were searched for common shared homozygous intervals from all affected family members using a custom script implemented in Mathematica (B.M., unpublished). This script identifies all homozygous intervals longer than 2 Mb for which there are no more than 1% heterozygous calls (to permit potential genotyping errors).

Mutation screening. Mutation screening for *CEP41* was performed by direct sequencing of the 11 coding exons and the adjacent intronic junctions in human subjects. The PCR products that were generated were treated with Exonuclease I (Fermentas) and shrimp alkaline phosphatase (SAP) (Promega), and both strands were sequenced using a BigDye Terminator v3.1 sequencing kit with an ABI3100 automated sequencer (Applied Biosystems). Information about the primers and the optimized PCR conditions used are provided in **Supplementary Table 3**. Segregation of the identified mutations was investigated in all available family members. None of the identified mutations in *CEP41* were found in 96 ancestrally matched controls (188 chromosomes) upon direct sequencing.

Bioinformatics. Genetic location is according to the March 2006 Human Genome Browser build hg18. The ciliary proteome was searched using web-based tools^{41,42}. Protein sequence conservation was determined using ClustalW multiple amino acid sequence alignment (see URLs).

Cloning. Full-length human *CEP41* was cloned into the TOPO Zero Blunt vector (Invitrogen), and shuttled into EGFP- and HA- encoding vectors. Human and zebrafish *CEP41* ORFs were amplified by RT-PCR and cloned into the pCS2+ vector in order to synthesize RNA for injection into zebrafish embryos. Mouse *Cep41* (a gift from A.T. Look) was amplified and cloned into the GST-, EGFP- and FLAG-encoding vectors for biochemical assays.

Generation of *Cep41* mutant mice. The Sanger Institute Gene Trap Resource (SIGTR) ES cell line (AW0157), derived from 129P2/OlaHsd mice carrying a gene-trap insertion⁴³ in intron 1 of *Cep41*, was obtained from the European Conditional Mouse Mutagenesis Program (EUCOMM) and injected into C57BL/6 recipient blastocysts at the Mouse Biology Program, University of California, Davis. High-percentage chimeras ($\geq 70\%$) were bred to C57BL/6 mice for germline transmission. Gene-trapped mice were isolated by PCR for the β -galactosidase-neomycin fusion gene and genotyped by Southern blot analysis, with hybridization of ~ 10 -kb (wild-type allele) or ~ 8 -kb (gene-trapped allele) products (**Supplementary Fig. 5**).

Zebrafish experiments. AB wild-type zebrafish strains (ZFIN) were used for *in situ* hybridization carried out by standard protocols using digoxigenin (DIG)-labeled sense and antisense RNA probes for *cep41*. To knock down zebrafish *cep41*, we used a translation-blocking MO (Gene Tools), 5'-CATCTTCCAGC AGCAGAGCTTCGGC-3', which was diluted to appropriate concentrations in

deionized sterile water and injected into embryos at the one-cell or two-cell stage, which were obtained from natural spawning of zebrafish lines. To rescue the phenotypes in MO-injected embryos, we co-injected RNA transcribed *in vitro* with the SP6 mMessage mMachine kit (Ambion). For characterization of ciliary defects in zebrafish embryos, the morphological phenotype of either *cep41* or *ttll6* morphants were observed until 5 days post-fertilization (d.p.f.) and quantified under bright-field microscopy based on previously established criteria⁴⁴. For protein blot analysis at 1–2 d.p.f., zebrafish control embryos and *cep41* morphants (~ 50 embryos with each genotype) were deyolked, and the embryos were lysed with RIPA buffer. For immunostaining, mouse antibody to acetylated-tubulin (Sigma), mouse antibody to GT335 (a gift from C. Janke) and rabbit PolyE antibody (a gift from M. Gorovsky) were used. Whole-mount zebrafish embryos, control embryos at 3 d.p.f. and *cep41* morphants were fixed in Dent's fixative (80:20 methanol:DMSO) at 4 °C overnight and incubated with primary antibody to GT335 (1:400), acetylated tubulin (1:400) or PolyG (1:300) and with anti-goat-mouse 594 (1:1,000, Life Technologies) secondary antibody in blocking solution diluted 1:2 (10% normal goat serum and 0.5% Tween-20 in PBS).

Cell culture and transfection. IMCD3, hTERT-RPE1, human fibroblasts and human embryonic kidney cells (HEK293) were grown in appropriate DMEM or MEM supplemented with 10–20% fetal bovine serum (FBS) at 37 °C in 5% CO₂. Control fibroblasts from healthy human females and males were obtained from the American Type Culture Collection (ATCC), and subject fibroblasts were isolated from skin biopsies and were propagated in culture (≤ 5 passages). Human fibroblasts were transfected using the Basic Nucleofector Kit for Primary Mammalian Fibroblasts (Lonza). Other cells were transfected at 60–80% confluency with plasmids or siRNA (see **Supplementary Table 4**) using Lipofectamine 2000 (Invitrogen). The transfected cells were incubated for 24–72 h with FBS or without FBS, dependent on the experimental purpose.

Fluorescence microscopy and transmission electron microscopy. Images of immunofluorescently stained cells were obtained on a Deltavision RT Deconvolution microscope (Olympus IX70) under the same parameters for each experiment. Acquired images were edited and analyzed using Adobe Photoshop CS. For electron microscopy, a standard protocol⁴⁵ was used except for the modification that tannic acid was included in the fixative to enhance the final contrast of the images. Formvar-coated slot grids (Electron Microscopy Sciences) were used for sections (60–70 nm) to maximize visibility of the tissue and cross-sectioning performed to observe cilia axonemal structure.

Live imaging of zebrafish embryos. Zebrafish embryos (12 h.p.f. for cilia in Kupffer's vesicle and 2.5 d.p.f. for the renal cilia) were transferred with their medium to glass-bottomed culture dishes (MatTek), and embryos at 2.5 d.p.f. were anesthetized in tricaine solution (~ 0.016 mg/ml). Images were acquired for 30s to 2 min intervals using a PerkinElmer UltraView Vox Spinning Disk Confocal microscope with EMCCD Hamamatsu 14 bit 1K \times 1K camera and edited with Volocity imaging software (PerkinElmer).

Immunofluorescence and biochemical assays. For immunofluorescence, cells were fixed in 100% methanol at -20 °C for 10 min. Primary antibodies used for immunofluorescence were: rabbit antibody to CEP41, raised in rabbit to a purified bacterially expressed GST-fused CEP41 protein (PRF&L), mouse antibody to acetylated-tubulin, mouse antibody to GT335, rabbit PolyE antibody and rabbit antibody to ARL13B (a gift from T. Caspary). We used Alexa 488- or Alexa 594-conjugated secondary antibodies (Molecular Probes) and Hoechst 33342 nuclear dye. All antibodies were diluted in 4% normal donkey serum in PBS. Primary antibodies were incubated with samples overnight at 4 °C and secondary antibodies were applied for 1 h at room temperature. For immunoblotting, cells were lysed with RIPA buffer 3 d after transfection and boiled with SDS sample buffer. Equal amounts of lysate were loaded for paired experiments. Primary antibodies used for protein blotting were: rabbit antibody to GFP (Roche), mouse antibody to Flag (Sigma) and mouse antibody to α -tubulin (Sigma). Bound antibodies were detected using horseradish peroxidase-conjugated secondary antibodies (Pierce). For co-immunoprecipitation, WCEs were prepared from confluent HEK293 cells transiently transfected with 14 μ g of plasmid DNA in 10-cm² tissue culture dishes. WCE supernatants

were processed for immunoprecipitation experiments by using 2 µg of primary antibody and protein A/G mixed agarose beads (Pierce).

Statistical analysis. The χ^2 statistic was computed manually with the *P* value assigned for 1 degree of freedom in the characterization of the mouse embryonic phenotype (**Supplementary Table 2**). For other studies, Student's two-tailed non-paired *t* tests were carried out to determine the statistical significance of differences between samples. *P* < 0.05 was considered statistically significant for all tests.

38. Valente, E.M. *et al.* Distinguishing the four genetic causes of Jouberts syndrome-related disorders. *Ann. Neurol.* **57**, 513–519 (2005).
39. Murray, S.S. *et al.* A highly informative SNP linkage panel for human genetic studies. *Nat. Methods* **1**, 113–117 (2004).
40. Hoffmann, K. & Lindner, T.H. easyLINKAGE-Plus—automated linkage analyses using large-scale SNP data. *Bioinformatics* **21**, 3565–3567 (2005).
41. Inglis, P.N., Boroevich, K.A. & Leroux, M.R. Piecing together a ciliome. *Trends Genet.* **22**, 491–500 (2006).
42. Gherman, A., Davis, E.E. & Katsanis, N. The ciliary proteome database: an integrated community resource for the genetic and functional dissection of cilia. *Nat. Genet.* **38**, 961–962 (2006).
43. Schnütgen, F. *et al.* Genomewide production of multipurpose alleles for the functional analysis of the mouse genome. *Proc. Natl. Acad. Sci. USA* **102**, 7221–7226 (2005).
44. Valente, E.M. *et al.* Mutations in *TMEM216* perturb ciliogenesis and cause Joubert, Meckel and related syndromes. *Nat. Genet.* **42**, 619–625 (2010).
45. Majumdar, A. & Drummond, I.A. Podocyte differentiation in the absence of endothelial cells as revealed in the zebrafish avascular mutant, cloche. *Dev. Genet.* **24**, 220–229 (1999).